Research Square

Preprints are preliminary reports that have not undergone peer review.
They should not be considered conclusive, used to inform clinical practice,
or referenced by the media as validated information.

Oculomics and Automated Retinal Microvasculature Analysis: Applications for Thalamic Microvascular Lesions

Constantin Geis

constantingeis@gmail.com

George Emil Palade University of Medicine, Pharmacy, Science, and Technology of Targu Mures

Márta Germán-Salló

George Emil Palade University of Medicine, Pharmacy, Science, and Technology of Targu Mures

Beáta Baróti

County Emergency Clinical Hospital of Targu Mures, Targu Mures

Tünde Pál

George Emil Palade University of Medicine, Pharmacy, Science, and Technology of Targu Mures

Zoltán Preg

George Emil Palade University of Medicine, Pharmacy, Science, and Technology of Targu Mures, Targu Mures

Enikő Nemes-Nagy

George Emil Palade University of Medicine, Pharmacy, Science, and Technology of Targu Mures

Henrik Haba

Iuliu Haţieganu University of Medicine and Pharmacy

Lajos Csincsik

School of Medicine, Dentistry and Biomedical Sciences, Queen's University Belfast

Robert G. Tripon

George Emil Palade University of Medicine, Pharmacy, Science, and Technology of Targu Mures

---

Research Article

Keywords: AutoMorph, oculomics, retinal microvasculature, central retinal arteriolar equivalent, fractal dimension, thalamic microvascular lesions

Posted Date: June 15th, 2026

DOI: https://doi.org/10.21203/rs.3.rs-9931287/v1

License: This work is licensed under a Creative Commons Attribution 4.0 International License.
Read Full License

Additional Declarations: No competing interests reported.

Abstract

This study aims to identify retinal vascular parameters in patients with thalamic microvascular lesions and to examine their association with lesion size. A further objective is to encourage implementation of open-source analytical platforms, such as AutoMorph and ImageJ, within oculomics and the evaluation of thalamic microvascular lesions; therefore, a detailed, step-by-step user guide is provided to facilitate their practical application. This retrospective study included 42 patients with arterial hypertension and thalamic microvascular lesions, as quantitatively assessed from magnetic resonance imaging scans using ImageJ. A total of 84 digital fundus photographs were analysed to evaluate microvascular morphological changes using AutoMorph software. Statistical analyses were performed in R using generalized estimating equation models with thalamic microvascular lesion size as the predictor and retinal vascular parameters as outcome variables, adjusted for age and sex, with significance set at $P < 0.05$. Following image quality control assessment, the final cohort comprised 28 participants and 44 fundus photographs. Significant associations were observed between thalamic microvascular lesion size and retinal vascular parameters. Greater lesion size was inversely associated with central retinal arteriolar equivalent (CRAE) in zone B ($\beta = -1.27$, $P = 0.040$) and zone C ($\beta = -1.24$, $P = 0.048$), as well as with artery vessel density ($\beta = -0.0004$, $P < 0.001$) and fractal dimension ($\beta = -0.001$, $P = 0.012$). Male participants exhibited larger CRAE values than females, while age showed no significant effect. Retinal artificial intelligence-based automated microvascular analysis shows potential as a non-invasive marker of thalamic microvascular lesions.

Introduction

In the course of embryonic development, both the retina and the optic nerve are derived from the diencephalon. Therefore, both structures are part of the central nervous system (CNS) [1]. The thalamus, as part of the diencephalon and a key relay station, possesses a variety of properties depending on the nucleus involved, such as arousal, mood, nociception, sensory, motor, and cognitive functions [2]. Thus, in cases of pathology, the signs and symptoms vary depending on the affected vascular territory [2].

The retinal microvasculature is composed of non-fenestrated endothelial cells and pericytes. Its structural integrity is crucial for maintaining the inner blood-retina barrier (BRB), which functions analogous to the blood brain barrier function [1]. Both the retina and the brain present comparable neural and microvascular characteristics [3]. With chronic arterial hypertension, the retinal microvasculature is damaged, and the vessel wall thickens, leading to an increased wall to lumen ratio [4]. In the brain, underlying mechanisms of cerebral small vessel disease (CSVD) due to arterial hypertension include arteriolosclerosis and lipohyalinosis, where smooth muscle cells proliferate, then degenerate, and are eventually replaced by fibroblasts and collagen. This process results in sclerosis and a decreased vessel lumen diameter, leading to reduced organ tissue perfusion [5]. The small perforating vessels supplying the thalamus, which are typically affected by lipohyalinosis, range from 40–300 μm [5]. Retinal arterioles vary between 50–100 μm [6], emphasizing the structural homology between both systems.

Given the similarities in embryonic origin, structural characteristics, arteriolar size, and shared pathophysiological processes, the retina may present a window into thalamic small vessel pathology. The following retinal vascular parameters have been associated with a variety of systemic vascular conditions and neurological diseases. Fractal dimension is a parameter that expresses the overall ramification complexity of the retinal vasculature and was found to be reduced in patients with lacunar stroke and white matter lesions [7–9]. Vessel density describes the degree of retinal vessel occupation in relation to the measured area and arterial vessel density can be decreased in CSVD [10]. Vascular tortuosity depicts how much the vessels twist and turn along the trajectory of the vessel [8]. Increased tortuosity is connected to multiple systemic cardiovascular conditions like coronary heart disease, peripheral artery disease, atherosclerosis, and hypertension [11]. The central retinal arteriolar equivalent (CRAE) and central retinal venular equivalent (CRVE) quantify the average calibre of arterioles, respectively venules, in a predetermined region peripapillary [12, 13]. An increased venular calibre and decreased arteriolar calibre are associated with an increased risk for atherosclerotic cardiovascular events [12]. A reduced CRAE is connected to arterial hypertension, lacunar infarction, Diabetes mellitus, Alzheimer's disease, glomerulonephropathy, and albuminuria [12, 14, 15].

To investigate these retinal parameters in the context of thalamic pathology, we utilized AutoMorph. AutoMorph is a fully automated open-source deep learning-based software pipeline that quantitatively analyses retinal vessel morphology [16].

This study aims to investigate the association between morphological retinal vascular biomarkers, measured on colour fundus images using AutoMorph, and thalamic microvascular lesion size assessed on MRI.

Furthermore, we aim to expand the clinical application of AutoMorph within the field of oculomics by presenting a comprehensive step-by-step guide to facilitate its practical use and a step-by-step ImageJ protocol for thalamic application.

Methods

This retrospective study analysed 42 patients diagnosed with thalamic microvascular lesions and concomitant arterial hypertension, confirmed by prior cardiology evaluation. All patients underwent cerebral MRI scans, using the GE Optima MR450w (1.5 Tesla) system, at the Radiology and Medical Imaging Laboratory - County Emergency Clinical Hospital of Targu Mures. A detailed step-by-step description of image analysis using ImageJ is provided in Online Resource 1.

Digital fundus photography was performed using a Carl Zeiss Visucam 500 fundus camera at the Ophthalmology clinic in Targu Mures, Romania. A total of 84 digital fundus photographs, comprising disc-centred and macula-centred images, were initially analyzed using AutoMorph. These images were processed using AutoMorph, and a step-by-step guide is provided in Online Resource 2. The software's built-in quality control module automatically excluded images that did not meet the technical standards.

After quality control, images of both eyes of 16 patients (32 fundus images) and one eye of 12 patients (12 fundus images) were included. The final dataset consisted of 44 fundus images from 28 patients.

Retinal vascular parameters, including calibre (CRAE and CRVE (using the revised Parr-Hubbard formula)), vessel density, vessel width, fractal dimension, tortuosity of arterioles and venules, were automatically generated for zone B and C by the algorithm. Zones B and C are defined as concentric regions relative to the optic disc. Zone B refers to 0.5 to 1 optic disc diameters distance from the disc margin, and zone C refers to 0.5 to 2 optic disc diameters distance from the disc margin and readily used in retinal vessel segmentation software such as SIVA (see Fig. 1) [13, 16, 17].

Quantitative manual analysis of thalamic microvascular lesion size was performed from cerebral MRI scans using ImageJ software. The hyperintense lesion area and the total thalamic area were measured in pixels, and thalamic microvascular lesion size (TML size, %) was calculated as the percentage of thalamic area occupied by hyperintense lesions. Lesions were categorized into small and large lesion groups based on the median TML size (%). All compiled data were imported into “R” (Version 4.4.2) for visualisation and statistical analysis. For the cohort characteristics table, normality of continuous variables was assessed using the Shapiro–Wilk test and group comparisons were performed using two-sample t-tests. Continuous variables are shown as mean (SD) and range, and categorical variables as n (%). For categorical comparisons, chi-square or Fisher’s test was applied. Generalized estimating equation (GEE) models, adjusted for age and sex, were employed to assess associations between retinal vascular parameters (dependent variables) and thalamic lesion size (independent variable), accounting for inter-eye correlations. Statistical significance was set at $P < 0.05$. Complete GEE model analyses of significant and non-significant results are listed in Online Resource 3.

Results

The final dataset comprised 44 fundus images from 28 patients aged 59 to 79 years, with a mean age of 70 years (SD = 4.34); 52% of observations were from female patients. Baseline characteristics and retinal vascular parameters stratified by thalamic microvascular lesion size are shown in Table 1. GEE analyses were performed to investigate the relationship between the degree of microvascular lesions in the thalamus and various retinal vascular parameters (RVP).

While several parameters showed directional trends graphically, indicative of microvascular alterations, such as reduction in arteriolar width, and vein vessel density, and increases in both arteriolar tortuosity, venular width and CRVE across both zone B and zone C, these associations did not reach statistical significance ($P > 0.05$). Notably, CRAE in zone B and C, artery vessel density, and fractal dimension presented a statistically significant inverse association with thalamic microvascular lesion size. Specifically, a one percentage-point increase in TML size corresponded to an estimated decrease of approximately 1.27 pixels in CRAE in Zone B (β = -1.27, 95% *CI*: -2.48 to -0.06, $P = 0.04$) and 1.24 pixels in CRAE Hubbard Zone C (β = -1.24, 95% *CI*: -2.46 to -0.01, $P = 0.048$). Sex also demonstrated a relationship with CRAE in zone B and C. Male participants had, on average, a greater CRAE in Zone B (β = 16.52, 95%

CI: 0.52 to 32.53, *P* = 0.043) and in Zone C (*β* = 18.19, 95% *CI*: 0.21 to 36.18, *P* = 0.047) than female participants. Age did not show significant associations with CRAE in this model (*P* > 0.05). Both artery vessel density (*β* = -0.0004, 95% *CI*: -0.0006 to -0.0002, *P* < 0.001) and fractal dimension (*β* = -0.001, 95% *CI*: -0.002 to -0.0003, *P* = 0.012) showed a statistically significant reduction with concomitant one percentage-point increase in TML size, however, with a smaller magnitude. The corresponding GEE model results for CRAE in zones B and C are shown in Tables 2 and 3, respectively. The GEE model results for artery vessel density and fractal dimension are shown in Tables 4 and 5, respectively.

Table 1

Dataset Characteristics Table showing demographics, TML size (%) and all examined RVPs for the total cohort and by TML size (small and large). Abbreviations: TML, thalamic microvascular lesion expressed as percentage of total thalamic area; CRVE, Central Retinal Venular Equivalent; CRAE, Central Retinal Arteriolar Equivalent. *P < 0.05 indicates statistical significance.

Variable	Total cohort	Large lesion	Small lesion	*P*-value
Age	69.70 (4.34), 59.00–79.00	70.24 (4.66), 62.00–79.00	69.22 (4.08), 59.00–75.00	0.44
Sex	female 23 (52.3%); male 21 (47.7%)	female 9 (42.9%); male 12 (57.1%)	female 14 (60.9%); male 9 (39.1%)	0.37
TML size (%)	6.68 (5.53), 1.35–24.59	10.81 (5.47), 5.57–24.59	2.9 (1.21), 1.35–5.33	-
Fractal Dimension	1.48 (0.03), 1.44–1.53	1.47 (0.03), 1.44–1.52	1.49 (0.02), 1.46–1.53	0.038*
Artery Vessel Density	0.03 (0.00), 0.02–0.04	0.03 (0.01), 0.02–0.04	0.03 (0.00), 0.03–0.04	0.004*
Artery Average Width	88.47 (5.77), 78.70–102.64	86.91 (5.64), 78.70–98.21	89.90 (5.63), 78.98–102.64	0.08
Artery Distance Tortuosity	5.49 (3.62), 1.13–15.64	5.41 (4.62), 1.13–15.64	5.56 (2.47), 1.16–9.97	0.89
Vein Vessel Density	0.04 (0.01), 0.03–0.05	0.04 (0.01), 0.03–0.05	0.04 (0.00), 0.03–0.05	0.29
Vein Average Width	103.89 (8.51), 80.94–121.16	103.85 (8.28), 89.23–117.68	103.92 (8.89), 80.94–121.16	0.97
Vein Distance Tortuosity	4.80 (2.91), 1.65–14.30	4.96 (3.03), 1.65–11.99	4.66 (2.86), 2.04–14.30	0.74
CRAE Hubbard Zone B	231.95 (25.22), 177.87–298.16	223.47 (23.43), 177.87–282.28	239.69 (24.76), 198.84–298.16	0.031*
CRAE Hubbard Zone C	247.27 (26.33), 187.00–302.41	240.09 (28.00), 187.00–302.41	253.84 (23.42), 213.60–296.92	0.08
CRVE Hubbard Zone B	299.99 (34.13), 218.98–374.29	300.93 (35.20), 251.07–374.29	299.13 (33.90), 218.98–344.37	0.86
CRVE Hubbard Zone C	328.18 (37.26), 232.78–406.45	330.83 (39.64), 265.98–406.45	325.75 (35.68), 232.78–378.88	0.65

Table 2

GEE Model Results – CRAE Zone B Generalized estimating equation model with TML size (%) as predictor and CRAE Zone B as outcome variable, including age and sex as covariates. Abbreviation: CI, Confidence Interval. *P < 0.05 indicates statistical significance.

CRAE Zone B	**Estimate**	**Standard Error**	**95% *CI* Lower**	**95% *CI* Upper**	***P*-Value**
TML size (%)	-1.266	0.61	-2.47	-0.05	0.04*
Age	-0.452	0.77	-1.97	1.07	0.56
Sex (Male = 1, Female = 0)	16.523	8.16	0.51	32.53	0.043*

Table 3

GEE Model Results – CRAE Zone C Generalized estimating equation model with TML size (%) as predictor and CRAE Zone C as outcome variable, including age and sex as covariates. *P < 0.05 indicates statistical significance.

CRAE Zone C	**Estimate**	**Standard Error**	**95% *CI* Lower**	**95% *CI* Upper**	***P*-Value**
TML size (%)	-1.236	0.62	-2.46	-0.009	0.048*
Age	-0.141	0.88	-1.87	1.59	0.87
Sex (Male = 1, Female = 0)	18.192	9.17	0.20	36.17	0.047*

Table 4

GEE Model Results – Artery Vessel Density Generalized estimating equation model with TML size (%) as predictor and Vessel Density artery (VDa) as outcome variable, including age and sex as covariates. *P < 0.05 indicates statistical significance.

VDa	**Estimate**	**Standard Error**	**95% *CI* Lower**	**95% *CI* Upper**	***P*-Value**
TML size (%)	-0.0004	0.0001	-0.0006	-0.0002	< 0.001*
Age	0.00003	0.0001	-0.0002	0.0003	0.79
Sex (Male = 1, Female = 0)	0.003	0.001	-0.00004	0.006	0.053

Table 5

GEE Model Results – Fractal Dimension

FD	**Estimate**	**Standard Error**	**95% *CI* Lower**	**95% *CI* Upper**	***P*-Value**
TML size (%)	-0.001	0.0006	-0.002	-0.0003	0.012*
Age	-0.0004	0.0008	-0.002	0.001	0.62
Sex (Male = 1, Female = 0)	0.005	0.009	-0.01	0.02	0.53

Generalized estimating equation model with TML size (%) as predictor and Fractal Dimension (FD) as outcome variable, including age and sex as covariates. *P < 0.05 indicates statistical significance.

Complete model results, including non-significant associations for other retinal microvascular parameters, are presented in Online Resource 3.

Discussion

In this study, we identify for the first time - to our knowledge - an association between quantitatively assessed retinal microvasculature morphology, using AutoMorph, and thalamic microvascular lesion size. Given that retinal microvasculature is easily accessible for non-invasive imaging, our findings suggest that retinal changes, particularly the reduction of CRAE, could serve as a potential biomarker for thalamic microangiopathy and cerebral small vessel disease (CSVD) progression. This reduced arteriolar calibre, as measured by CRAE, may reflect underlying systemic microvascular dysfunction. Our observation that reduced CRAE in Zone B and C correlates with thalamic lesions aligns with established mechanisms of hypertensive microangiopathy. Chronic arterial hypertension affects the cerebral vessels by focal arteriolar constriction that in turn causes a decrease in blood supply to the tissue with subsequent development of ischemic lesions [18]. Similarly, chronic arterial hypertension induces vascular remodelling and generalized arteriolar narrowing in the retinal vasculature [19]. Specific modifications include an increase in size of the intima, hyperplasia of the media, and vessel wall sclerosis [19]. These parallel modifications imply that CRAE, as an indicator of retinal arteriolar calibre, may mirror analogous pathological processes occurring in the cerebral microvasculature. Underlying pathophysiological mechanisms of CSVD include an increase in thickness of the vessel wall, endothelial cell dysfunction, activation of microglia, gliosis, and alteration of the blood-brain-barrier [20]. These processes are likely to contribute to chronic hypoperfusion and tissue damage, especially in deep brain structures such as the thalamus.

The inverse relationship between thalamic lesion size and CRAE (Zone B and C) supports this shared pathophysiology. Systemic hypertension likely drives arteriolar narrowing in both the retina and small perforating arteries supplying deep cerebral territories like the thalamus. Since thalamic microvascular pathology, including ischemia, can produce a wide range of symptoms depending on the affected vessel and involved territory [3], early detection of retinal microvascular changes, if confirmed in larger longitudinal cohorts, could be particularly valuable in identifying high-risk patients before the onset of symptoms.

Our findings complement and extend prior observations of decreased retinal nerve fibre layer (RNFL) and ganglion cell-inner plexiform layer (GCIPL) thickness in thalamic infarction [3]. While these earlier studies identified structural neurodegeneration via SS-OCT and vascular density reductions in the SVP/ICP via OCTA [3], our work suggests a parallel microvascular mechanism: arteriolar narrowing (reduction in CRAE), a lower artery vessel density, and a decrease in fractal dimension, limiting blood flow to retinal neuronal tissue. This hypoperfusion may contribute to the RNFL/GCIPL thinning in thalamic infarction.

Our analyses revealed a significant CRAE reduction in both Zones B and C, indicating peripapillary microvascular dysfunction. Furthermore, the statistically significant decrease in fractal dimension as sign of less complex vessel ramification and artery vessel density, showing decreased vessel occupation per area of retinal tissue, may additionally contribute to the retinal hypoperfusion. Graphical regression showed consistent directional trends (all $P > 0.05$) for: reduced venular density and arteriolar width and increased arteriolar tortuosity, venular width, and CRVE across both zones B and C.

A previous study reported similar retinal microvascular changes in association with stroke; however, these investigations did not specifically focus on thalamic stroke. The retinal parameters commonly linked to stroke include wider retinal venular diameter, narrower arteriolar diameter, increased overall vessel tortuosity, and reduced fractal dimension [21]. Furthermore, the reduction of CRAE and the increase in CRVE were found to be connected to lacunar ischemia [14]. From a pathophysiological perspective, fractal dimension was shown to be in relationship with hypoxia, further supporting our findings that a reduced fractal dimension is connected to thalamic ischemia, whereas an increase in vascular tortuosity was associated with vascular wall impairment and loss of blood retina barrier integrity [14].

Our results highlight CRAE narrowing in retinal fundus images as a potential surrogate marker for identifying microvascular pathology in the thalamus associated with CSVD.

Several limitations of this study need to be discussed. First, due to the cross-sectional design and the absence of a control group, causal interpretations of the observed associations cannot be made. Longitudinal studies are required to investigate whether retinal vessel alterations precede or result from CSVD. Second, the sample size in our study was reduced from 84 fundus photographs to 44 fundus photographs, due to the failure to pass the image quality grading module of the AutoMorph software. Therefore, results need to be confirmed and further assessed with a larger sample size. Given the exploratory nature of this study, the results should be interpreted as hypothesis-generating and require validation in independent cohorts. Lastly, confounding factors like hypertension need to be accounted for in future studies, as they can influence both retinal and thalamic microvasculature. Despite these limitations, our findings provide further evidence for future studies into retinal biomarkers of thalamic microvascular pathology.

Conclusion

Non-invasive imaging of the retina with automated analysis of vascular morphology could serve as a surrogate marker for the detection of cerebral microvascular pathology. Retinal microvasculature changes and their role as a surrogate for thalamic lesions, such as the decrease of the arteriolar calibre, arterial vessel density, and fractal dimension, need to be further validated in larger cohorts over time.

Declarations

Competing interests:

The authors have no relevant financial or non-financial interests to disclose.

Ethical approval:

Ethical approval no. 19779 was granted by the Ethics Committee of the County Emergency Clinical Hospital of Targu Mures. All participants were informed about the study's purpose and procedures, and consent was obtained prior to inclusion. The research was carried out in compliance with the principles outlined in the Declaration of Helsinki regarding medical studies involving human subjects.

Consent to participate:

All participants were informed about the purpose and procedures of the study, informed consent was obtained and participation was voluntary.

Consent for publication:

Not applicable.

Funding:

This study received funding from the Hungarian Academy of Sciences and the Studium Prospero Foundation through a shared grant (grant no. 346).

Author Contribution

Conceptualization: Robert G. Tripon, Lajos Csincsik, Márta Germán-Salló; Methodology: Constantin Geis, Lajos Csincsik, and Robert G. Tripon; Data collection: Robert G. Tripon, Márta Germán-Salló, Beáta Baróti, Tünde Pál, Zoltán Preg, Enikő Nemes-Nagy, and Henrik Haba; MRI analysis: Henrik Haba; Retinal image analysis: Constantin Geis; Formal analysis: Constantin Geis; Writing—original draft preparation: Constantin Geis; Writing—review and editing: Constantin Geis, Lajos Csincsik, Robert G. Tripon, Márta Germán-Salló, Beáta Baróti, Tünde Pál, Zoltán Preg, Enikő Nemes-Nagy, and Henrik Haba. All authors read and approved the final manuscript.

Acknowledgement

The authors express their gratitude to the Head of department, Associate professor Karin U. Horvath, for facilitating patient evaluations at the Ophthalmology Clinic of Targu Mures, and to Dr. Norbert Lita for his valuable assistance in preparing the supplementary material.

Data availability:

The datasets generated or analyzed during the current study are not publicly available due to patient privacy and institutional data protection regulations but are available from the corresponding author on reasonable request and subject to approval by the responsible institutional authorities.

References

1. DeBuc DC, Somfai GM, Koller A (2017) Retinal microvascular network alterations: Potential biomarkers of cerebrovascular and neural diseases. Am. J. Physiol. Heart Circ. Physiol. 312:H201–H212. https://doi.org/10.1152/ajpheart.00201.2016
2. Schmahmann JD (2003) Vascular syndromes of the thalamus. Stroke 34:2264–2278. https://doi.org/10.1161/01.STR.0000087786.38997.9E
3. Ye C, Kwapong WR, Tao W, et al (2022) Characterization of Macular Structural and Microvascular Changes in Thalamic Infarction Patients: A Swept-Source Optical Coherence Tomography-Angiography Study. Brain Sci 12 (5):518. https://doi.org/10.3390/brainsci12050518
4. Gallo A, Mattina A, Rosenbaum D, et al (2016) Retinal arteriolar remodeling evaluated with adaptive optics camera: Relationship with blood pressure levels. Ann Cardiol Angeiol (Paris) 65:203–207. https://doi.org/10.1016/j.ancard.2016.04.021
5. Lammie GA (2002) Hypertensive cerebral small vessel disease and stroke. In: Brain Pathology. International Society of Neuropathology, pp 358–370
6. Cogan DG, Kuwabara T, Friedman E (1968) Retinal vasculature. Microvasc Res 1:115–132. https://doi.org/10.1016/0026-2862(68)90012-5
7. Lemmens S, Devulder A, Van Keer K, et al (2020) Systematic Review on Fractal Dimension of the Retinal Vasculature in Neurodegeneration and Stroke: Assessment of a Potential Biomarker. Front Neurosci 14:16. https://doi.org/10.3389/fnins.2020.00016
8. Hilal S, Ong YT, Cheung CY, et al (2014) Microvascular network alterations in retina of subjects with cerebral small vessel disease. Neurosci Lett 577:95–100. https://doi.org/10.1016/j.neulet.2014.06.024
9. McGrory S, Ballerini L, Doubal FN, et al (2019) Retinal microvasculature and cerebral small vessel disease in the Lothian Birth Cohort 1936 and Mild Stroke Study. Sci Rep 9:6320. https://doi.org/10.1038/s41598-019-42534-x
10. Wang D, Wang L, Wang J, et al (2024) Retinal structure and vessel density changes in cerebral small vessel disease. Front Neurosci 18:1288380. https://doi.org/10.3389/fnins.2024.1288380
11. Tomasoni M, Beyeler MJ, Vela SO, et al (2023) Genome-wide Association Studies of Retinal Vessel Tortuosity Identify Numerous Novel Loci Revealing Genes and Pathways Associated With Ocular and Cardiometabolic Diseases. Ophthalmology science 3:100288. https://doi.org/10.1016/j.xops.2023.100288

12. Hanssen H, Streese L, Vilser W (2022) Retinal vessel diameters and function in cardiovascular risk and disease. Prog. Retin. Eye Res. 91:101095. https://doi.org/10.1016/j.preteyeres.2022.101095
13. Gao Y, Xu L, He N, et al (2023) A narrative review of retinal vascular parameters and the applications (Part I): Measuring methods. Brain Circ 9:121–128. https://doi.org/10.4103/bc.bc_8_23
14. Rim TH, Teo AWJ, Yang HHS, et al (2020) Retinal Vascular Signs and Cerebrovascular Diseases. Journal of Neuro-Ophthalmology 40:44–59. https://doi.org/10.1097/WNO.0000000000000888
15. Geerling CF, Terheyden JH, Langner SM, et al (2022) Changes of the retinal and choroidal vasculature in cerebral small vessel disease. Sci Rep 12:3660. https://doi.org/10.1038/s41598-022-07638-x
16. Zhou Y, Wagner SK, Chia MA, et al (2022) AutoMorph: Automated Retinal Vascular Morphology Quantification Via a Deep Learning Pipeline. Transl Vis Sci Technol 11(7):12. https://doi.org/10.1167/tvst.11.7.12
17. Cheung CYL, Hsu W, Lee ML, et al (2010) A new method to measure peripheral retinal vascular caliber over an extended area. Microcirculation 17:495–503. https://doi.org/10.1111/J.1549-8719.2010.00048.X
18. Lassen NA, Agnoli A (1972) The upper limit of autoregulation of cerebral blood flow - on the pathogenesis of hypertensive encephalopathy. Scand. J. Clin. Lab. Invest. 30:113–116. https://doi.org/10.3109/00365517209081099
19. Wong TY, Mitchell P (2004) Hypertensive Retinopathy. New England Journal of Medicine 351:2310–2317. https://doi.org/10.1056/NEJMra032865
20. Abdelhak A, Huss A, Brück A, et al (2020) Optical coherence tomography-based assessment of retinal vascular pathology in cerebral small vessel disease. Neurol Res Pract 2:13. https://doi.org/10.1186/s42466-020-00062-4
21. Ong YT, De Silva DA, Cheung CY, et al (2013) Microvascular structure and network in the retina of patients with ischemic stroke. Stroke 44:2121–2127. https://doi.org/10.1161/STROKEAHA.113.001741

Figures

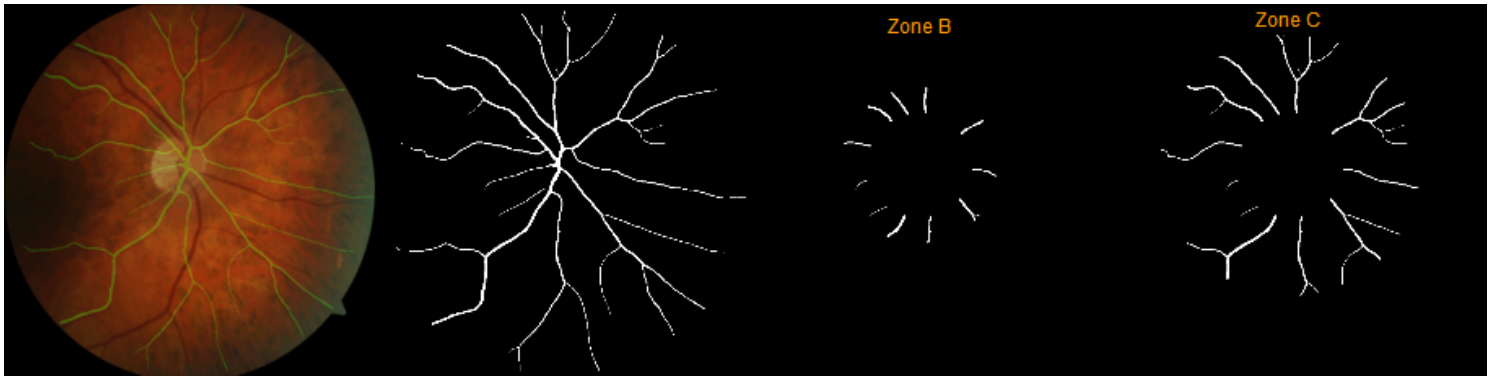


Figure 1

AutoMorph artery vessel segmentation images from the right eye. From left to right: original fundus image with green colour overlay on arteries, binary arterial vasculature overall, binary arteries in Zone B and binary arteries in Zone C

Supplementary Files

This is a list of supplementary files associated with this preprint. Click to download.

- OnlineResource1.pdf
- OnlineResource2.pdf
- OnlineResource3.pdf